

Geophysical Research Letters

RESEARCH LETTER

10.1002/2015GL064100

Key Points:

- Ocean isopycnal mixing is uncertain
- This uncertainty can produce order 20% variation in anthropogenic carbon uptake
- Values in boundary currents appear to matter most

Supporting Information:

- Data set S4
- Data set S3
- Data set S2
- Data set S1
- Figure S1

Correspondence to:

A. Gnanadesikan,
gnanades@jhu.edu

Citation:

Gnanadesikan, A., M.-A. Pradal, and R. Abernathey (2015), Isopycnal mixing by mesoscale eddies significantly impacts oceanic anthropogenic carbon uptake, *Geophys. Res. Lett.*, 42, 4249–4255, doi:10.1002/2015GL064100.

Received 4 APR 2015

Accepted 11 MAY 2015

Accepted article online 14 MAY 2015

Published online 2 Jun 2015

Isopycnal mixing by mesoscale eddies significantly impacts oceanic anthropogenic carbon uptake

Anand Gnanadesikan¹, Marie-Aude Pradal¹, and Ryan Abernathey²

¹Department of Earth and Planetary Sciences, Johns Hopkins University, Baltimore, Maryland, USA, ²Department of Earth and Environmental Sciences, Columbia University, New York, New York, USA

Abstract Anthropogenic carbon dioxide uptake varies across Earth System Models for reasons that have remained obscure. When varied within a single model, the lateral eddy mixing coefficient A_{Redi} produces a range of uptake similar to the modeled range. The highest uptake, resulting from a simulation with a constant A_{Redi} of 2400 m²/s, simulates 15% more historical carbon uptake than a model with $A_{\text{Redi}} = 400$ m²/s. A sudden doubling in carbon dioxide produces a 21% range in carbon uptake across the models. Two spatially dependent representations of A_{Redi} produce uptake that lies in the middle of the range of constant values despite predicting very large values in the subtropical gyres. One-dimensional diffusive models of the type used for integrated assessments can be fit to the simulations, with A_{Redi} accounting for a substantial fraction of the effective vertical diffusion. Such models, however, mask significant regional changes in stratification and biological carbon storage.

1. Introduction

By taking up approximately one quarter of the carbon emitted by human activities each year, the ocean plays an important role in slowing the rate of global warming but at the cost of decreasing pH and calcite supersaturation. The latest round of simulations done for the Intergovernmental Panel on Climate Change process produce estimates of anthropogenic carbon inventory in 1995 ranging from 87 Gt C to 112 Gt C, a range of 29% [Frohlicher *et al.*, 2014]. The reasons for this range remain unclear, as different models have different representations of ocean physics and biological cycling, as well as different responses to historical climate forcing. One aspect of ocean physics where climate models show little consensus is the representation of lateral mixing along density surfaces by mesoscale eddies.

Lateral eddy mixing is often characterized in terms of a turbulent diffusion coefficient A_{Redi} [Redi, 1982]. In most of the current generation of models this describes diffusion along isopycnal surfaces in the ocean interior and in the horizontal in the mixed layer, producing fluxes which go as $F_C = -A_{\text{Redi}} \nabla_h C$, where $\nabla_h C$ represents the lateral tracer gradient. It is distinguished from the Gent-McWilliams coefficient A_{GM} , which parameterizes the eddy form drag associated with mesoscale eddies [Gent and McWilliams, 1990]. This form drag generates advective tracer fluxes of the form $F_C = -A_{\text{GM}} \partial S / \partial z \times C$, where S is the isopycnal slope. A number of models follow previous theoretical work [Green, 1970; Stone, 1972; Visbeck *et al.*, 1997] which postulates that both eddy diffusivities scale as the growth rate of mesoscale eddies multiplied by the square of the width of the zone in which density surfaces slope steeply. Such parameterizations produce a distribution of A_{Redi} which generally follows that shown in Figure 1a: A_{Redi} is high in boundary currents where density surfaces slope and low in the gyres, and very high latitudes and low latitudes where density surfaces are flat. Such a pattern is consistent with the idea that eddy mixing should track eddy kinetic energy. Such models (which include the National Center for Atmospheric Research Community Earth System Model, Geophysical Fluid Dynamics Laboratory (GFDL) ESM2G, and NorESM models) predict depth-averaged values of a few hundreds of m²/s in the gyres and values ranging from around 650 to 1500 m²/s in the boundary currents [Gnanadesikan *et al.*, 2006; Danabasoglu *et al.*, 2012; Dunne *et al.*, 2012; Bentsen *et al.*, 2013].

Observations, however, give a very different picture. Estimates from tracers [Ledwell *et al.*, 1998; Gnanadesikan *et al.*, 2013] and floats [Lumpkin and Flament, 2001] range from around 1000 m²/s to upward of 10,000 m²/s. One recent estimate [Abernathey and Marshall, 2013] uses satellite altimetry to generate an eddy velocity field, which is then used to advect tracers with the resulting fields being inverted for diffusivity. The resulting diffusion coefficient (Figure 1b), which represents cross-frontal mixing, has a structure that is substantially different from that in Figure 1a with higher values in the gyres and lower values in boundary currents.

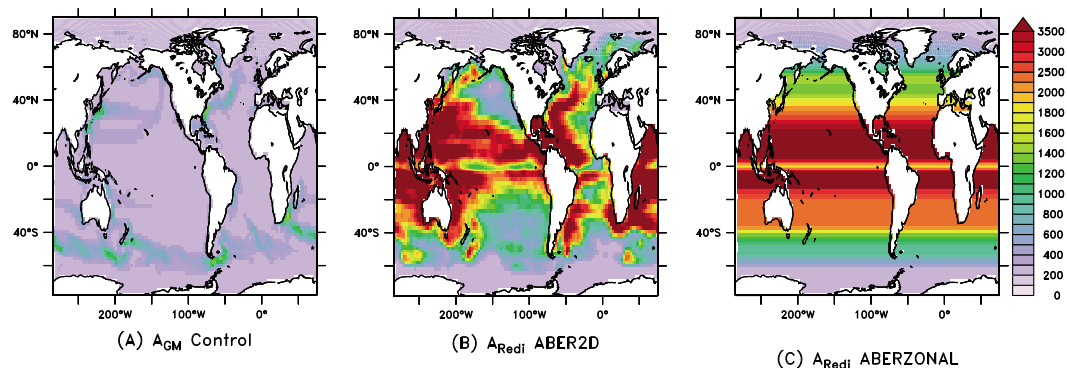


Figure 1. Mixing coefficients in $\text{m}^2 \text{s}^{-1}$ in the climate model suite. (a) A_{GM} coefficient in the control run, showing high values in the boundary currents and lower values in the interior. (b) A_{Reidi} from Abernathay and Marshall [2013] used in ABER2D simulation. (c) Zonally averaged version of field in Figure 1b used in ABERZONAL simulation.

None of the current generation of climate models uses a distribution of A_{Reidi} like that in Figure 1b. Some models effectively split the difference between Figures 1a and 1b by using constant values ranging from $500 \text{ m}^2/\text{s}$ in the Hadley center model [Jones et al., 2011] and $600 \text{ m}^2/\text{s}$ in the GFDL ESM2M model [Dunne et al., 2012] to $2000 \text{ m}^2/\text{s}$ in the CMCC model [Fogli et al., 2009]. Often this is done to tune surface properties such as RMS error in sea surface temperature within a model that does not contain biogeochemical cycling [Gnanadesikan et al., 2006].

This paper shows that the uptake of anthropogenic carbon depends on the choice of A_{Reidi} . In section 2, we describe a set of sensitivity studies with an Earth System Model that we use to evaluate this dependence. Section 3 shows that anthropogenic carbon uptake can vary substantially across these models and that the impacts of changing mixing can be well approximated by using a simple one-dimensional model. Section 4 concludes this paper.

2. Model Description

Our physical model is the GFDL ESM2Mc, a coarse-resolution version of the ESM2M [Galbraith et al., 2011] model reported in Dunne et al. [2012]. This model consists of a $3.875 \times 3^\circ$ atmosphere with 24 vertical levels, essentially a coarse version of the model used in the Fourth Assessment Report. The ocean model in ESM2M has a nominal resolution of $3 \times 1.5^\circ$ resolution and 28 levels in the vertical. The model is non-Boussinesq, using a pressure rather than a Cartesian vertical coordinate and thus conserves mass and is able to handle greater thickness of sea ice than previous versions of the GFDL model. The vertical diffusivity in the model is the sum of a background diffusivity of $1 \times 10^{-5} \text{ m}^2/\text{s}$ and a tidally driven diffusion following Simmons et al. [2004]. The advective effect of eddies is handled using a shear-dependent mixing coefficient A_{GM} , which yields the diffusion coefficients shown in Figure 1a. The advective flux associated with this coefficient is capped at $A_{\text{GM}} S_{\text{max}}$, where $S_{\text{max}} = 0.01$ to prevent unrealistically large velocities near mixed layers where slopes become infinite. We use a larger S_{max} than in the CM2.1 model allowing a more realistic deep overturning.

Biological cycling in ESM2Mc is handled using the Biology Light Iron Nutrients and Gasses model of Galbraith et al. [2010]. This model explicitly carries six tracers: dissolved inorganic carbon, alkalinity, micronutrient, macronutrient, dissolved organic material, and oxygen. Phytoplankton growth rates are computed using the simulated light (which depends on the chlorophyll concentration within the water column), micronutrient, and macronutrient. Following the theory of Dunne et al. [2005], these growth rates are then used to create a highly parameterized ecosystem that matches observations of the partitioning of biomass between large and small phytoplankton and the corresponding fraction of productivity exported as particulate organic material. The model has a complex cycle of micronutrient, involving deposition from dust, adsorption onto sinking particles, remineralization, and a sedimentary source. When forced with observed atmospheric fluxes, the model produces distributions of surface macronutrient and chlorophyll comparable to those associated with models with many more explicit tracers. Because the biology is prognostic, the BLING model can simulate changes to natural biological carbon pumps that arise from climate variability and change.

A spin-up was made in which the model was initialized using observations of temperature, salinity, and nutrients and run with “preindustrial” (year 1860) levels of greenhouse gases and aerosols for 1500 years. The A_{Redi} coefficient for this run was set to 800 m²/s and the run is referred to as AREDI800. At year 1500, perturbation runs with four different values of A_{Redi} were branched off the main trunk and allowed to run for 360 years. Three runs with constant values of $A_{\text{Redi}} = 400, 1200,$ and $2400 \text{ m}^2/\text{s}$ are referred to as AREDI400, AREDI1200, and AREDI2400, respectively. For clarity of exposition, we will focus on the AREDI400 and AREDI2400 cases in the figures here; however, the AREDI800 and AREDI1200 cases lie neatly between the two. Additionally, we make a run with the spatially dependent distribution of *Abernathay and Marshall* [2013] shown in Figure 1b which rises as high as 5500 m²/s in the subtropical gyres but drops to very low values in the Southern Ocean. We refer to this simulation as ABER2D. Because this estimate depends on the observed flow field, it may be inconsistent with the model climate and cannot be easily applied to paleoclimates. We, therefore, conducted an additional set of simulations with a zonally averaged version of this parameterization, denoted ABERZONAL and shown in Figure 1c.

At year 1860, three further sets of runs were spun off the suite. First, the controls with constant CO₂ were extended for an additional 140 years. *Historical CO₂* simulations were performed in which the CO₂ was allowed to follow its historical trajectory with respect to the air-sea fluxes but not to affect the radiation. Atmospheric CO₂ is taken from the Siple dome ice core before 1990 (following the OCMIP2 protocol) but from a global atmospheric data set from 1990 to 2000 (following the OCMIP3 protocol). This change in data source results in a significant change in the interannual variability after 1990 which shows up in the air-sea fluxes. Each Historical CO₂ run produces an identical circulation as the corresponding control, allowing us to calculate the passive uptake of anthropogenic carbon dioxide while ignoring feedbacks on circulation. We chose this approach because a true historical run has impacts not only from carbon dioxide, but from other radiatively active trace gasses as well. Finally, *Doubling CO₂* runs were made in which the atmospheric carbon dioxide was doubled to a value of 572 ppmv for both the carbon and radiation schemes. This allows us to separate the passive impact of increasing CO₂ on solubility from the active impact that changing CO₂ would have on circulation and the associated biological and solubility carbon pumps.

3. Results

Historical anthropogenic carbon uptake varies significantly across the model suite both for the globe (Figure 2a) and most especially for the Southern Ocean (Figure 2b). The range of air-sea carbon fluxes in the final decade of the simulation spans a range of 2.22–2.55 Gt C/yr. This compares with observational estimates (with a nominal date of 1995) of 1.9 ± 0.6 [Manning and Keeling, 2006] estimated from O₂/N₂ ratios in air and 2.2 ± 0.6 Gt C/yr [Mikaloff-Fletcher et al., 2006] from a joint inversion of atmospheric and oceanic data. As in *Frohlicher et al.* [2014], the models show less of a range than the uncertainty of observational estimates, making it impossible to use these estimates to place strong constraints on oceanic mixing. The model with the highest constant mixing coefficient (AREDI2400) shows the highest air-sea flux, about 15% higher than the model with the lowest constant mixing coefficient (AREDI400) and just outside of the O₂/N₂ ratio-based estimates. These differences are dominated by the Southern Ocean, where AREDI2400 shows 29% more uptake than AREDI400 south of 30°S (1.01 Gt C/yr versus 0.79 Gt C/yr). While it might be expected that the very high values of mixing coefficient in the ABER2D and ABERZONAL models would lead to an even higher uptake, these models lie in between the two constant cases, with an air-sea flux of 2.42 Gt C/yr and 2.44 Gt C/yr, respectively, over the final decade over the globe as a whole and 0.88 and 0.90 in the Southern Ocean. The fact that $A_{\text{Redi}} < 1000 \text{ m}^2\text{s}^{-1}$ south of 48°S is apparently more important than the very high values found in the gyre interior. All the uptake curves are much smoother than the raw air-sea fluxes, indicating that most of the interannual variance in the raw air-sea flux is due to natural variability.

The total inventory of anthropogenic carbon in 1995 (Figure 2d) mirrors the uptake results, with AREDI2400 giving 118.7 Gt C while AREDI400 simulates 102.7 Gt C and ABER2D gives 112 Gt C. Anthropogenic carbon uptake simulations without physical feedbacks are thus able to produce a range of uptake that is about half of the range simulated in the CMIP5 models, with our estimates generally lying on the high end of the model range. Observational estimates of anthropogenic carbon have been made using hydrography, differing in the method used to estimate the baseline carbon concentration. *Sabine et al.* [2004] use the Global Ocean Data Analysis Project data set to find an uptake (excluding coastal regions, the Mediterranean and the Arctic and waters below 2000 m) of 106 ± 17 Gt C at a nominal year of 1995. When we make similar assumptions, our inventories range between 88 and 99 Gt C, somewhat lower than the observational estimates but with

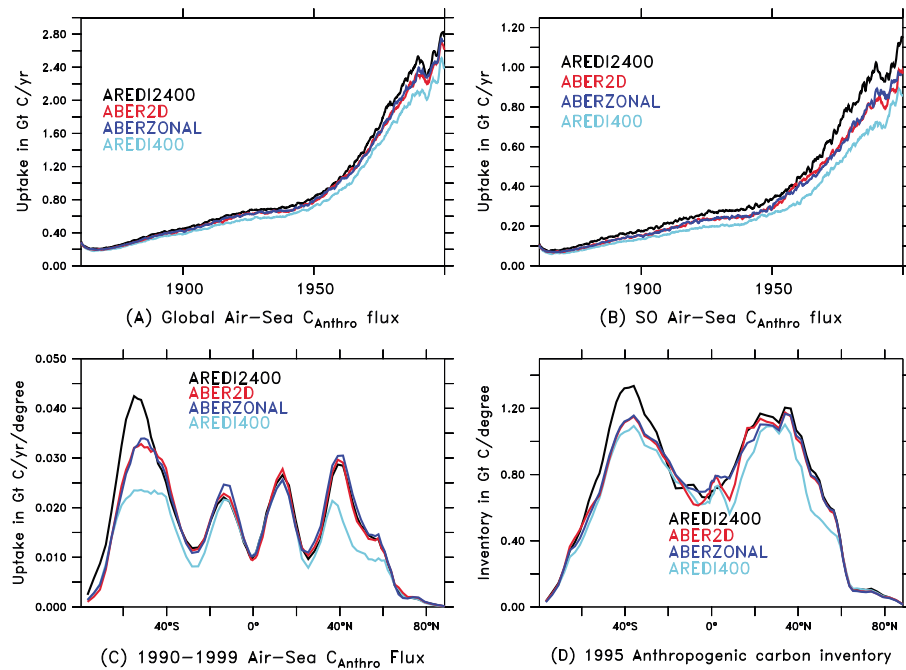


Figure 2. Anthropogenic carbon as a function of lateral mixing. The highest-mixing case (AREDI2400) is shown in black, the lowest (AREDI400) in light blue, and the cases with mixing given by the fields in Figures 1b and 1c (ABER2D and ABERZONAL) in red and dark blue respectively. (a) Global air-sea anthropogenic carbon flux from 1860 to 2000 in Gt C/yr. (b) Southern Ocean anthropogenic carbon flux from 1860 to 2000 in Gt C/yr. (c) Zonally integrated anthropogenic carbon flux in Gt/yr/deg. (d) Zonally integrated carbon inventory averaged from 1990 to 2000 in Gt/deg.

the upper values lying well within the error bars. Similarly, our values lie at the lower end of the range of 94–122 Gt C estimated by Waugh *et al.* [2006] assuming that the transport of water from the ocean surface to the interior occurs over a range of pathways with different transit times.

Including physical and biological feedbacks from increasing carbon dioxide does not change the qualitative picture that emerges from the historical runs. As shown in Figure 3, the spatial distribution of anthropogenic carbon 100 years after doubling is well correlated with the historical distribution with coefficients ranging between 0.93 and 0.95. In AREDI400, the dominant storage is in the gyres and North Atlantic. The higher mixing cases, however, produce more storage in the North Pacific, as increased isopycnal mixing destabilizes the halocline there and allows old waters to come to the surface and take up anthropogenic carbon. Under climate change, the relative range in uptake across models increases relative to the historical suite, with AREDI400 predicting a total inventory of 438 Gt C, while AREDI2400 predicts an inventory of 530 Gt C (21% higher). Again the ABER2D model lies in the middle of the pack, with an inventory of 493 Gt C, in between the AREDI800 and AREDI1200 cases (with uptakes of 464 and 494 Gt C, respectively). The ABERZONAL model (not shown) has an almost identical uptake of 498 Gt C/yr. While historical uptake is a good predictor of future uptake, the indirect impacts of CO₂ on circulation magnify the differences between the different models.

For many years, estimates of future uptake of anthropogenic carbon dioxide in integrated assessment models have been made using a one-dimensional diffusion equation

$$\frac{\partial C}{\partial t} = K_v^{\text{eff}} \frac{\partial^2 C}{\partial z^2} \quad (1)$$

where K_v^{eff} is a diffusion coefficient that parameterizes not only diapycnal vertical diffusion but also lateral transport from gyres and eddies along sloping isopycnal surfaces [Oeschger *et al.*, 1975]. In the specific case of step CO₂ doubling, such an equation predicts that the anthropogenic carbon burden should equal $\Delta C_{\text{surf}} A_{\text{ocean}} \sqrt{K_v^{\text{eff}} t}$ where ΔC_{surf} is the mean change in surface concentration (118 mmol/m³ for doubling) A_{ocean} is the area of the ocean and t is time. The rate of increase of anthropogenic carbon after doubling (Figure 4a) is very smooth and (Figure 4b) fits a square root curve very well, validating the one-dimensional approach. Inverting for diffusion coefficients at $t = 100$ years, we get values of 2.23, 2.48, 2.81, and

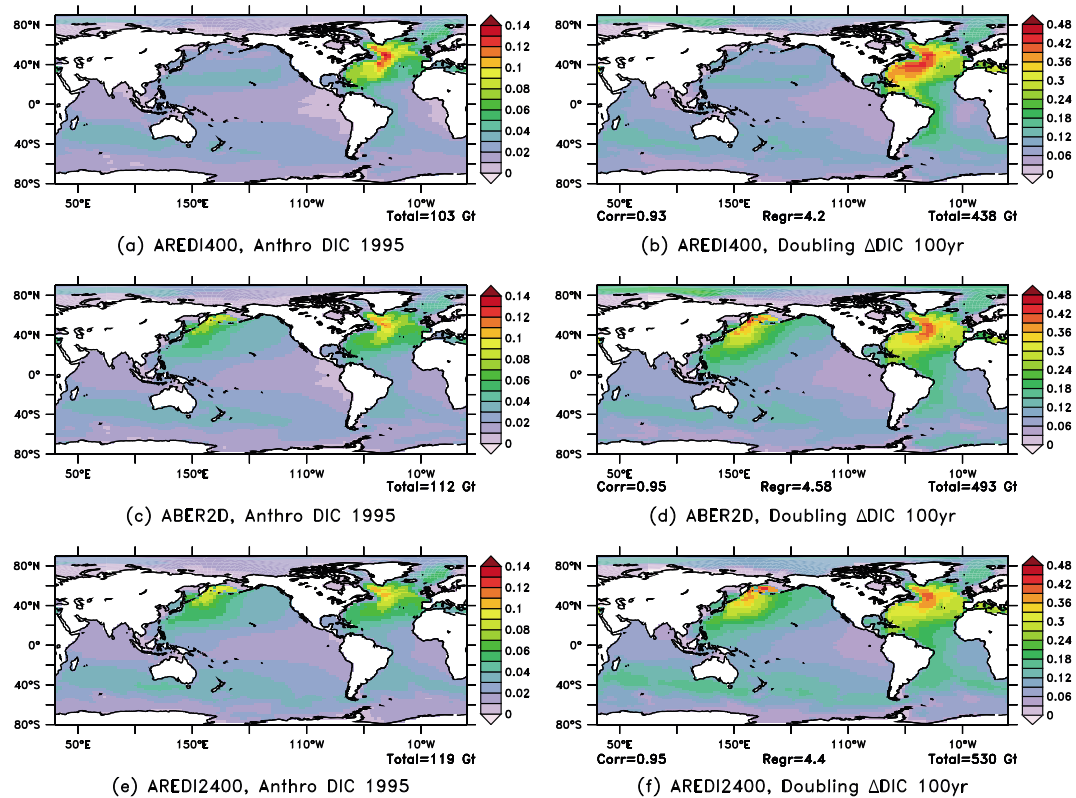


Figure 3. Comparison between historical (left) uptake of carbon in mol C/m² with no circulation change and (right) uptake of carbon from a sudden doubling of the concentration. (top) AREDI400 case (lowest mixing). (middle) ABER2D case. (bottom) AREDI2400 case (highest mixing).

3.26×10^{-4} m²/s for AREDI400, AREDI800, AREDI1200, and AREDI2400, respectively. When the model is applied to predict transient uptake, the results depend on the exact value of the air-sea transfer coefficient. Assuming that it takes 1 year to equilibrate the top 80 m, the AREDI400 value predicts mean burden from 1990 to 2000 of 101 Gt C while the AREDI2400 value predicts a mean anthropogenic burden from 1990 to 2000 of 122 Gt C. Both of these are reasonably close to the modeled values.

Are these values physically reasonable? Since the vertical diffusion due to mixing along a sloping isopycnal can be written [Redi, 1982] as $K_v = A_{\text{Redi}} S_p^2$, where S_p^2 is the square of the local isopycnal slope, the global average effective diffusion coefficient can then be written as $K_v = K_v^0 + A_{\text{Redi}} \bar{S}^2$, where the overbar denotes a

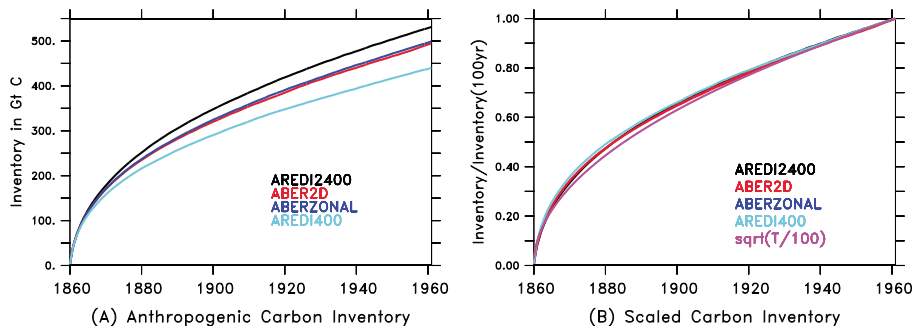


Figure 4. Inventory of anthropogenic carbon after instantaneous doubling. (a) Time series in Gt C versus year of model simulation (doubling starts at year 1860, so the year is 1860 + T). (b) Scaled inventory (inventory/inventory at $T = 100$ years). Also shown in magenta line is $\sqrt{T/100}$ years. The strong agreement between these lines suggest small impacts from differences in the base state of the models in carbon pumps in the model control states and interannual variability.

spatial average. Fitting the four constant mixing cases, we find a mean effective squared slope of 5.14×10^{-8} , corresponding to having about 4% of the global ocean covered with slopes of order 1/1000. Given that the fraction of the ocean where isopycnal slopes are higher than 1/1000 varies between 2% at 150 m and 10% at 500 m in the World Ocean Atlas data set, this result is physically reasonable. The results suggest that isopycnal mixing along tilted surfaces can play a significant role in vertical exchange in climate models. Even for the AREDI400 run, the contribution of isopycnal mixing along tilted surfaces to the effective vertical diffusion is $1.3 \times 10^{-5} \text{ m}^2/\text{s}$, similar to the background vertical diffusion due to breaking internal waves (suggesting that gyre transport contributes the largest amount). For the AREDI2400 run, it accounts for about one third of the effective vertical diffusion.

While the use of an effective vertical diffusion is computationally efficient, Figure 3 demonstrates that such a representation masks large regional differences in uptake. In particular, because increasing mixing tends to decrease stratification in the North Pacific, it tends to increase the overturning in this basin, with values for AREDI400, AREDI800, AREDI1200, and AREDI2400 being 4.1, 5.1, 14.5, and 18.5 Sv, and the values for ABER2D and ABERZONAL being 17.2 and 20.3 Sv, respectively. The higher values are associated with unrealistically high levels of radiocarbon and low levels of mantle helium in the deep North Pacific [Gnanadesikan *et al.*, 2014]. By contrast, the North Atlantic overturning is relatively stable across the runs at 19–21 Sv. While the overturning decreases under climate change, the high mixing cases show a larger decline in the Atlantic than do the low mixing cases, as reflected in the lower inventories of anthropogenic carbon in the Atlantic but unrealistically high inventories of anthropogenic carbon in the North Pacific.

Treating anthropogenic uptake as if it were completely controlled by the downward diffusion of atmospheric carbon also ignores the impact of changes in the biological pump. In the AREDI400 simulation, the preformed phosphate inventory decreases by 23 Tmol over 100 years and the resulting increase in remineralized carbon is 38 Gt, 5.8 Gt of which is associated with increased inventory of remineralized calcium carbonate. The remainder is close to the 29 Gt C which would be expected given the C:P ratio of 106 used in BLING. In AREDI2400, the decrease in preformed phosphate is 59 Tmol, and the increase in remineralized carbon is 89 Gt, 16 Gt of which is associated with increased remineralized calcium carbonate. Increased biological storage thus accounts for about half the difference between the highest and lowest mixing cases, even though it only accounts for about 7–12% of the overall carbon uptake.

4. Conclusions

Our results demonstrate that a better understanding of isopycnal mixing will be useful for generating projections of carbon feedbacks in the future. Eddy-resolving models that directly simulate this mixing [Ito *et al.*, 2010] will be able to capture changes associated with changes in winds and the location of fronts that fixed parameterizations will not. However, we note that resolving eddies requires resolutions of order 5 km, requiring several orders of magnitude more computational resources than the coarse models described here. Our results suggest that while modeling eddies will add confidence to our estimates of anthropogenic uptake, it will not produce a picture that is fundamentally different from the coarser runs.

Because our climate models are far from perfect, boundary currents and convective regions are often offset for observations. As a result, using fixed distributions of A_{Redi} as in ABER2D and ABERZONAL, likely produces unrealistic mixing in such regions, particularly if the zone of high mixing overlaps the boundary current rather than lying on one side of it. This likely explains the unrealistically large overturning in the North Pacific. We believe it is essential to develop dynamical models of mixing that can be run at coarser resolution and capture both the three-dimensional structure of mixing and its response to changes in the large-scale hydrography. Our results also offer the promise that more frequent and accurate estimation of carbon uptake with time may be able to place stronger constraints on isopycnal mixing than have hitherto been possible.

Our results contrast with Mignone *et al.* [2006] who looked at the impact on anthropogenic carbon uptake of increasing $A_{\text{GM}} = A_{\text{Redi}}$ together across a suite of models. They showed that increasing eddy mixing in this manner acts to shallow the low-latitude pycnocline and that anthropogenic carbon uptake was well correlated with the global mean pycnocline depth. However, when $A_{\text{Redi}} \neq A_{\text{GM}}$, increasing A_{Redi} causes the global mean pycnocline depth to decrease slightly (though much less than for changing A_{GM} by comparable amount, Figure S1 in the supporting information), even as the total uptake increases (Figure 2). This suggests that increasing A_{GM} decreases how much water equilibrates with the atmosphere, while increasing A_{Redi} increases how rapidly this water equilibrates. The results of Mignone *et al.* [2006] show that the former effect is dominant

when the two are changed together, but our results suggest that the second effect is nontrivial when the two are changed separately. Further work distinguishing these effects is clearly required.

Acknowledgments

Support for A.G. and M.A.P. was provided under NSF grants EAR-1135382 and OCE-1338814 and DOE grant SC0007066. Support for R.A. was provided by NASA grant NNX14AI46G. Data are provided in four files in the supporting information.

The Editor thanks two anonymous reviewers for their assistance in evaluating this paper.

References

- Abernathey, R., and J. Marshall (2013), Global surface eddy diffusivities derived from satellite altimetry, *J. Geophys. Res. Oceans*, **118**, 901–916, doi:10.1002/jgrc.20066.
- Bentsen, M., et al. (2013), The Norwegian Earth System Model, norESM1-M- Part 1: Description and basic evaluation of the physical climate, *Geosci. Model Dev.*, **6**, 687–720.
- Danabasoglu, G., S. C. Bates, B. P. Briegleb, S. R. Jayne, M. Jochum, W. G. Large, S. Peacock, and S. G. Yeager (2012), The CCSM4 ocean component, *J. Clim.*, **25**, 1361–1389.
- Dunne, J. P., R. A. Armstrong, A. Gnanadesikan, and J. L. Sarmiento (2005), Empirical and mechanistic models of particle export, *Global Biogeochem. Cycles.*, **19**, GB4026, doi:10.1029/2004GB002390.
- Dunne, J. P., et al. (2012), GFDL's ESM2 global coupled climate-carbon earth system models part I: Physical formulation and baseline simulation characteristics, *J. Clim.*, **25**, 6646–6665.
- Fogli, P., E. Manzini, M. Vichi, A. Alessandri, L. Patara, S. Gualdi, E. Scoccimaro, S. Masina, and A. Navarra (2009), INGV-CMCC Carbon (ICC): A carbon cycle Earth System Model, *Tech. Rep. No. 61*, Centro Euro–Mediterraneo per i Cambiamenti Climatici, Bologna.
- Frohlicher, T., J. L. Sarmiento, D. J. Paynter, J. P. Dunne, J. P. Krasting, and M. Winton (2014), Dominance of the Southern Ocean in anthropogenic carbon and heat uptake in CMIP5 models, *J. Clim.*, **28**, 862–886, doi:10.1175/JCLI-D-14-00117.1.
- Galbraith, E. D., A. Gnanadesikan, J. P. Dunne, and M. R. Hiscock (2010), Regional impacts of iron-light colimitation in a global biogeochemical model, *Biogeosciences*, **7**, 1043–1064.
- Galbraith, E. D., et al. (2011), Climate variability and radiocarbon in the CM2Mc Earth System Model, *J. Clim.*, **24**, 4230–4254, doi:10.1175/2011JCLI3919.1.
- Gent, P., and J. C. McWilliams (1990), Isopycnal mixing in ocean models, *J. Phys. Oceanogr.*, **20**, 150–155.
- Gnanadesikan, A., et al. (2006), GFDLs CM2 global coupled climate models-Part 2: The baseline ocean simulation, *J. Clim.*, **19**, 675–697.
- Gnanadesikan, A., D. Bianchi, and M. A. Pradal (2013), Critical role of mesoscale eddy diffusion for supplying oxygen to hypoxic ocean waters, *Geophys. Res. Lett.*, **40**, 5168–5174, doi:10.1029/2013GL057674.
- Gnanadesikan, A., R. Abernathey, and M. A. Pradal (2014), Exploring the isopycnal mixing and helium-heat paradoxes in a suite of Earth System Models, *Ocean Sci. Discuss.*, **11**, 2343–2367.
- Green, J. S. (1970), Transfer properties of the large-scale eddies and the general circulation of the atmosphere, *Q. J. R. Meteorolog. Soc.*, **96**, 157–185.
- Ito, T., M. Woloszyn, and M. Mazloff (2010), Anthropogenic carbon dioxide transport in the Southern Ocean driven by Ekman flow, *Nature*, **463**, 80–83.
- Jones, C. D., et al. (2011), The HadGEM2-ES implementation of CMIP5 centennial simulations, *Geosci. Model Dev.*, **4**, 543–570, doi:10.5194/gmd-4-543-2011.
- Ledwell, J. R., A. J. Watson, and C. S. Law (1998), Mixing of a tracer in the pycnocline, *J. Geophys. Res.*, **103**(C10), 21,499–21,529.
- Lumpkin, R., and P. Flament (2001), Lagrangian statistics in the central North Pacific, *J. Mar. Syst.*, **29**, 141–155.
- Manning, A. C., and R. F. Keeling (2006), Global oceanic and land biota sinks from the Scripps atmospheric oxygen flask sampling network, *Tellus B*, **58**, 95–116.
- Mikaloff-Fletcher, S. E., et al. (2006), Inverse estimates of anthropogenic CO₂ uptake, transport and storage by the ocean, *Global Biogeochem. Cycles.*, **20**, GB2002, doi:10.1029/2005GB002530.
- Mignone, B., A. Gnanadesikan, J. L. Sarmiento, and R. D. Slater (2006), Central role of Southern Hemisphere winds and eddies in modulating oceanic uptake of anthropogenic carbon dioxide, *Geophys. Res. Lett.*, **33**, L01604, doi:10.1029/2005GL024464.
- Oeschger, H., U. Siegenthaler, U. Schotterer, and A. Gugelmann (1975), A box diffusion model to study the carbon dioxide exchange in nature, *Tellus*, **27**, 168–192.
- Redi, M. H. (1982), Ocean isopycnal mixing by coordinate rotation, *J. Phys. Oceanogr.*, **12**, 1154–1157.
- Sabine, C. L., et al. (2004), The oceanic sink for anthropogenic CO₂, *Science*, **305**, 367–371.
- Simmons, H. L., S. R. Jayne, L. C. St. Laurent, and A. J. Weaver (2004), Tidally driven mixing in a numerical model of the ocean general circulation, *Ocean Model.*, **6**, 245–263.
- Stone, P. H. (1972), A simple radiative-dynamical model for the static stability of rotating atmospheres, *J. Atmos. Sci.*, **29**, 479–485.
- Visbeck, M., J. Marshall, T. Haine, and M. Spall (1997), Specification of eddy transfer coefficients in coarse-resolution ocean circulation models, *J. Phys. Oceanogr.*, **27**, 381–402, doi:10.1175/1520-0485(1997)027<0381:SOETCI>2.0.CO;2.
- Waugh, D. W., T. M. Hall, B. I. McNeil, R. M. Key, and R. J. Matear (2006), Anthropogenic CO₂ in the oceans estimated using transit-time distributions, *Tellus*, **58**, 376–390.